

# **CHARACTERIZATION OF CHEMICAL HETEROGENEITY IN POLYMER SYSTEMS USING HYDROLYSIS AND TAPPING MODE ATOMIC FORCE MICROSCOPY**

by

**D. Raghavan and X. Gu  
Polymer Science Division  
Department of Chemistry  
Howard University  
Washington DC 20059, USA**

and

**T. Nguyen and M. R. VanLandingham  
Building and Fire Research Laboratory  
National Institute of Standards and Technology  
Gaithersburg, MD 20899-8621, USA**

Reprinted from the *Journal of Polymer Science Part B: Polymer Physics*, Vol. 39, 1460-1470, 2001.

**NOTE:** This paper is a contribution of the National Institute of Standards and Technology and is not subject to copyright.



**NIST**

**National Institute of Standards and Technology**  
Technology Administration, U.S. Department of Commerce

# Characterization of Chemical Heterogeneity in Polymer Systems Using Hydrolysis and Tapping-Mode Atomic Force Microscopy

D. RAGHAVAN,<sup>1</sup> X. GU,<sup>1</sup> T. NGUYEN,<sup>2</sup> M. VANLANDINGHAM<sup>2</sup>

<sup>1</sup>Polymer Science Division, Department of Chemistry, Howard University, 525 College Street, Northwest, Room 120, Washington, DC 20059

<sup>2</sup>Building Materials Division, Building and Fire Research Laboratory, National Institute of Standards and Technology, Gaithersburg, Maryland 20899

*Received 2 November 2000; revised 28 March 2001; accepted 2 April 2001*

**ABSTRACT:** Characterization of polymer coatings microstructure is critical to the fundamental understanding of the corrosion of coated metals. An approach for mapping the chemical heterogeneity of a polymer system using chemical modification and tapping-mode atomic force microscopy (TMAFM) is demonstrated. This approach is based on the selective degradation of one of the phases in a multiphase polymer blend system and the ability of TMAFM to provide nanoscale lateral information about the different phases in the polymer system. Films made of a 70:30 polyethyl acrylate/polystyrene (PEA/PS) blend were exposed to a hydrolytic acidic environment and analyzed using TMAFM. Pits were observed to form in the PEA/PS blend films, and this degradation behavior was similar to that of the PEA material. Using these results, the domains in the 70:30 blend were identified as the PS-rich regions and the matrix as the PEA-rich region. This conclusion was confirmed by Fourier transform infrared-attenuated total reflection analyses that revealed the hydrolysis of the PEA material. TMAFM phase imaging was also used to follow pit growth of the blend as a function of exposure time. The usefulness of the chemical modification/AFM imaging approach in understanding the degradation process of a coating film is discussed. © 2001 John Wiley & Sons, Inc. *J Polym Sci Part B: Polym Phys* 39: 1460–1470, 2001

**Keywords:** atomic force microscopy; coatings; chemical modification; polymer heterogeneity; degradation

## INTRODUCTION

Organic coatings are widely used in buildings, bridges, aircrafts, automobiles, and electronic

equipment both for functional and aesthetic purposes. Depending on the application, the specifications of the organic coatings can vary over a wide range. Generally, a coating system is composed of a top coat, a primer, and a surface pretreatment. The role of a coating system is to provide protection against chemicals, moisture, and UV light.

Despite great improvements in coatings technology, problems still exist in the long-term protection of metals when exposed to aggressive environments.<sup>1</sup> Corrosion of polymer coated metals has been observed to occur only in certain regions

---

Certain commercial instruments and materials are identified in this article to adequately describe the experimental procedure. In no case does such identification imply recommendation or endorsement by the National Institute of Standards and Technology and Howard University, nor does it imply that the instruments or materials are necessarily the best available for the purpose.

*Correspondence to:* D. Raghavan (E-mail: draghavan@howard.edu)

*Journal of Polymer Science: Part B: Polymer Physics*, Vol. 39, 1460–1470 (2001)  
© 2001 John Wiley & Sons, Inc.

and not uniformly over the coated surface. The corroded regions are found to be directly beneath degradation-susceptible regions in the coating.<sup>2</sup> These degradation-susceptible regions are microscopic in dimension and have chemical, physical, and mechanical properties that are different from the rest of the film. Although they occupy only a small fraction of the film volume, they control the corrosion-protection performance of a polymer coating.<sup>2-4</sup> In recent years, research has been conducted to characterize the degradation-susceptible regions in coatings, but they have been limited to indirect measurements such as microhardness, DC resistance, and AC impedance.<sup>5,6</sup> The exact nature of these regions and the degradation mechanism are unknown. However, the behavior of these regions has been observed to be similar to that of a hydrophilic membrane, that is, they have a high ionic conductivity and high water-uptake capacity.<sup>3</sup> During exposure to aggressive environments, these regions are believed to undergo degradation, leading to the formation of conductive pathways through the film and allowing corrosive ions to reach the metal surface.<sup>7</sup> These regions are believed to consist of partially polymerized, low molecular weight, low-crosslinked materials and are not uniformly distributed in the polymer coating film.<sup>8</sup>

## BACKGROUND

Relating the microstructural features to the performance of coatings requires mapping and characterizing the degradation-susceptible regions, which have been the subject of much interest. For the mapping of heterogeneity in thin films, polymer blends and copolymers have served as useful model systems.<sup>9,10</sup> In the past, analytical techniques such as small-angle X-ray scattering, X-ray photoelectron spectroscopy, neutron scattering, and secondary ion-mass spectrometry have been widely used to provide valuable in-depth microstructural information of polymers.<sup>11-12</sup> However, these techniques provide limited capability to both visually and qualitatively characterize the surface morphology from the micron to the angstrom scale. Surface-morphology characterization of thin polymer film is essential because the surface properties influence the interactions that may occur between the film and the external environment. For example, the lateral composition on an exterior surface of a thin polymer film mostly defines the wettability of the material.<sup>13</sup>

Advances in a number of scanning probe microscopy techniques have made obtaining nanoscale lateral information of surfaces possible for polymeric materials.<sup>14-17</sup> Although scanning tunneling microscopy is effective for characterizing conducting materials, atomic force microscopy (AFM) is suited for examining nonconducting materials. AFM is a tool commonly used to image the topography of thin and thick films of organic and inorganic materials and biological molecules at high resolution under ambient conditions.<sup>18-20</sup> Novel imaging modes such as tapping-mode atomic force microscopy (TMAFM) have been developed to image surfaces of soft materials that are prone to tip-induced damages.<sup>21,22</sup> In TMAFM, the cantilever oscillates vertically near its resonance frequency so that the tip makes a brief contact with the sample during each oscillation cycle. The level of tapping force used during imaging is related to the ratio of the set-point amplitude to the free-oscillation amplitude, hereafter called the set-point ratio ( $r_{sp}$ ). As the tip is brought into contact with the sample surface, changes occur in the probe oscillation including phase angle, amplitude, and frequency as a result of tip-sample interactions. A phase image is recorded based on the changes in phase angle as a constant amplitude is maintained. Phase images for heterogeneous materials often reflect differences in the adhesive and/or mechanical properties of different phases or components.<sup>22-24</sup> However, interpretation of complex phase-image data to obtain individual properties has yet to be achieved.<sup>25</sup>

Force-mode AFM is a nonimaging mode in which the probe tip moves vertically with respect to the sample to measure the tip-sample interaction forces as a function of separation distance. The force curve obtained from the force mode has been used to provide localized information about adhesion, friction, and compliance of the sample. Careful use of this mode can be used to perform nanoscale indentation of polymers. Using a combination of force-mode and TMAFM, we have shown that it is possible to effectively map mechanically heterogeneous regions in multicomponent polymer systems.<sup>26,27</sup>

Although AFM techniques can provide nanoscale information of organic materials with regard to tip-sample adhesion and sample compliance, they provide only limited information, if any, about the chemical nature of different groups present at the surfaces. The development of chemical force microscopy (CFM) has opened new

possibilities to map chemically heterogeneous surfaces on a truly molecular scale.<sup>28</sup> Several groups have modified the tips and/or the samples used in AFM studies to map the chemically heterogeneous regions in a sample at the nanoscale level.<sup>28–31</sup> For this purpose, the AFM probe tips and sample substrates have been modified with a number of functional groups (e.g.,  $-\text{CH}_3$ ,  $-\text{NH}_2$ , and  $-\text{COOH}$ ) based on both siloxane and thiol model compounds. The former can react covalently with the Si ( $\text{SiO}_2$ ) tips and Si ( $\text{SiO}_2$ ) samples, whereas the latter can react with a gold layer that is deposited on the tip and/or substrate. Wong et al.<sup>32,33</sup> recently reported a major improvement in the lateral molecular imaging of surfaces when functionalized AFM probe tips were replaced by functionalized carbon nanotubes.

The CFM technique has been used to probe adhesion forces between chemical groups on the tip/nanotube and specific functional groups of the sample in organic and aqueous solvents. A measure of these forces provides a general basis for mapping the distribution of groups on lithographically patterned sample surfaces.<sup>29</sup> Because different regions of the lithographically patterned samples have the same chain length and microstructure, any measurement of force is attributed mainly to the chemical characteristics of the region. These patterned samples are regarded as model surfaces for the study of surface structures because they have regularly packed long alkyl chains.<sup>34,35</sup> In general, organic material (i.e., polymers) can have a very irregular packing of chains. In addition, polymers can have chain-length variations for the molecules present on the surface. The combination of chemical heterogeneity, irregular packing of chains, and chain-length variations can all contribute to the difficulty in the mapping of polymeric surfaces by CFM.<sup>36,37</sup>

A solvent-based method in combination with AFM was recently used to study chemically heterogeneous polymer surfaces.<sup>37</sup> The solvent-based method is applicable for studies of phase-separated structures if the phases have different degrees of swelling in a particular solvent. Elbs et al.<sup>37</sup> exploited this solvent-based AFM characterization method to investigate the characteristics of microdomains in triblock and diblock polymer systems. In the present study, an highly aggressive chemical medium has been chosen to effectively modify one component, keeping the other component unmodified. An inorganic acid has been chosen as the aggressive chemical medium

to accelerate the hydrolysis of one of the components in a two-component polymer blend.

The objectives of the current research are to identify heterogeneous regions in poly(ethyl acrylate) (PEA)/polystyrene (PS) blends using AFM and to study the progressive degradation of different components in a blend at the nanoscale by AFM. The second objective would be useful in understanding the degradation modes of organic coatings exposed to aggressive environments. In this article, TMAFM experiments are combined with a hydrolysis experiment to study the heterogeneity in polymer blends before and after exposure to HCl vapor. AFM results are used along with results from Fourier transform infrared spectroscopy (FTIR) to assist in interpreting the different regions in the chemically heterogeneous PEA/PS system.

If proven successful, the AFM/chemical modification approach would be useful for identifying different phases in chemically heterogeneous polymeric systems. Research in this area is still in its infancy. This approach is also helpful in providing a better understanding of the degradation of coating materials. This information is essential for developing better protective coatings against corrosion of metals.

## EXPERIMENTAL

### Materials

PEA with a weight-average molecular weight ( $M_w$ ) = 119,300 and a glass-transition temperature ( $T_g$ ) =  $-30$  °C and PS with  $M_w$  = 250,000 and  $T_g$  = 104 °C were acquired from the Aldrich Chemical Co. Blend 1 had mass fractions of both PEA and PS of 50% (hereafter designated as 50:50); Blend 2 had a mass fraction of PEA of 20% and a mass fraction of PS of 80% (hereafter designated 20:80); and Blend 3 had a mass fraction of PEA of 70% and a mass fraction of PS of 30% (hereafter designated 70:30). To prepare these blend samples, separate 2% mass-fraction solutions of PS and PEA in toluene were mixed in appropriate amounts. The three blends were cast into thin films by spin coating on silicon substrate, the details of which can be found elsewhere.<sup>26</sup> All of the cast films were conditioned for 24 h at  $24$  °C  $\pm$  2 °C before analysis. Some of the conditioned samples were analyzed using AFM, whereas the remaining samples were exposed to acid vapors.

In addition to the blend samples, cast films of PEA were prepared so that changes in the PEA-rich regions of the blend samples as a result of acid exposure could be compared to the changes in the pure PEA film. The cast PEA films were prepared using a mass fraction of 5% of PEA in toluene and the same spin-casting procedure as used for the blend films. For the FTIR study, the PEA film was solution-cast on a  $\text{CaF}_2$  substrate.

### Acid Hydrolysis

The cast PEA and PEA/PS films were exposed to 2-M HCl acid vapor by placing them on the desiccator's grid, which was kept several centimeters above the acid solution level. The hydrolysis experiment was conducted at  $24 \pm 2$  °C for up to 500 h. At specified time intervals, samples were removed from the closed desiccator and characterized by AFM and FTIR. Care was taken to image the same region of the sample before and after exposure by AFM and FTIR. The samples that were withdrawn from the desiccator for AFM and FTIR analyses were placed back in the chamber for future analyses. For the current investigation, the exposure time was defined as the time the sample was inside the HCl-containing desiccator.

### Atomic Force Microscopy

TMAFM was used to characterize the polymer blend samples. All AFM images were recorded with a Dimension 3100 scanning probe microscope from Digital Instruments operated under ambient conditions ( $24 \pm 2$  °C,  $45 \pm 5\%$  relative humidity) using microfabricated silicon cantilever probes. Manufacturer's values for the probe-tip radius and probe-spring constant were in the ranges of 5–10 nm and 20–100 N/m, respectively. Topographic and phase images were obtained simultaneously using a resonance frequency of approximately 300 kHz for the probe oscillation, a scan rate of 1 Hz, and a free-oscillation amplitude,  $A_0$ , of  $60 \pm 5$  nm. Typically, a set-point to free-amplitude ratio (rsp) of 0.50:0.75 was used in the experiments.

Film thicknesses were determined by AFM technique. To this end, a section of the film was removed with toluene to expose the bare silicon substrate, and the height of the remaining polymer film was determined relative to the underlying substrate. The result reported was the average of six measurements.

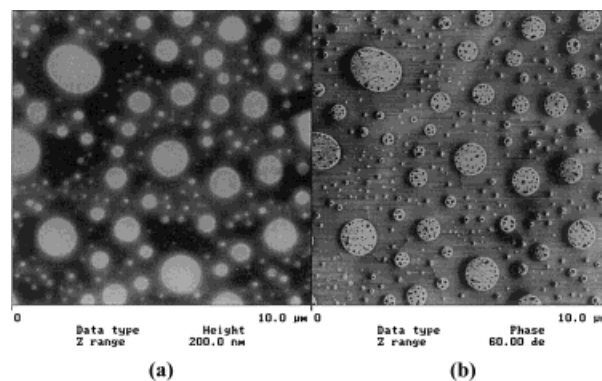


**Figure 1.** Tapping-mode AFM height image (left) and phase image (right) for the 70:30 PEA/PS blend after 24 h of ambient conditioning ( $r_{\text{sp}} = 0.70$ ). Contrast variations are 200 nm from white to black for the height images and  $60^\circ$  from white to black for the phase image.

### Fourier Transform Infrared Spectroscopy

FTIR transmission spectra of the cast PEA films on  $\text{CaF}_2$  before and after exposures to HCl vapor were collected using a Nicolet 560× FTIR spectrometer equipped with a mercury–cadmium–telluride detector. All spectra were acquired as 200 signal-averaged scans between 1200 and 3800  $\text{cm}^{-1}$  at a resolution of 4  $\text{cm}^{-1}$ . The peak heights of the carbonyl absorptions at 1732 and 1710  $\text{cm}^{-1}$  were used to express the ester and acid peak intensities, respectively. Dry air was used as the purge gas.

## RESULTS

### Unexposed PEA:PS Blends

In Figure 1(a), a two-dimensional topographic image (left) along with the corresponding phase image (right) are shown for a 70:30 blend film obtained by AFM under ambient conditions ( $r_{\text{sp}} = 0.70$ ). The magnification of these images is indicated by the scan dimension, which is 10  $\mu\text{m}$ . The thickness of this film was  $150 \pm 20$  nm, as measured by AFM. Both the phase and topographic images reveal that phase separation has occurred; the domains that appear as circular regions are of bright contrast with respect to the matrix. The domains are separated and have a typical size of 0.05–1.5  $\mu\text{m}$ . The size, dispersity, shape, and spacing of the domains vary over the sample surface. The lateral sizes of the domains in a polymer blend have been found to be strongly

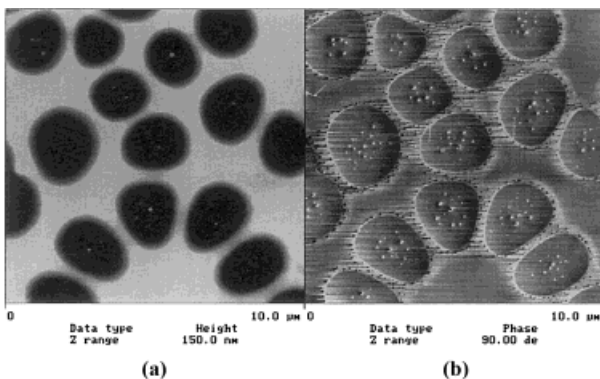


**Figure 2.** Tapping-mode AFM height image (left) and phase image (right) for the 50:50 PEA/PS blend after 24 h of ambient conditioning ( $r_{sp} = 0.75$ ). Contrast variations are 150 nm from white to black for the height image and  $90^\circ$  from white to black for the phase image.

influenced by the reduction in the mobility of polymer chains caused by solvent evaporation during spin coating.<sup>38</sup>

Within the domains are much smaller features that are a few nanometers in lateral dimension. In the topographic image, these smaller features are not evident, possibly because any associated topographic changes are small relative to those of the large structures. The smaller features in the phase image tend to have darker phase contrast compared with their surroundings, and this phase contrast is similar to that of the matrix material. This is particularly apparent in higher resolution phase images (not shown). Similar observations have been made in other two-component blend systems.<sup>23,26,27</sup> During spin coating, solvent evaporates from the polymer film, leaving behind two phases, one that is rich in polymer A and one that has a small amount of polymer A encapsulated in polymer B-rich material. As the solvent amount in the individual phase decreases as a result of solvent evaporation, the polymer diffusion coefficients are reduced to the extent where transport of polymer A over large distances becomes increasingly difficult.<sup>38</sup> Therefore, the regions of the major polymer component in a phase rich in the minor component are detected as nanodomains.

Several studies have assigned the domain and the matrix based on the topographic image contrast as a function of composition.<sup>39</sup> Using a similar approach, an attempt was made using the topographic results of 70:30, 50:50, and 20:80 blend films to assign the bright and dark regions

in the topographic image to PS or PEA in the blend. Figures 2 and 3 illustrate the AFM images [topographic (left) and phase (right)] of the 50:50 and 20:80 blend films after 24 h of ambient conditioning, respectively (AFM images of the 70:30 blend are given in Fig. 1). The phase data in Figure 2(a) shows an interesting ringlike structure around the topographically depressed domains. A similar ringlike structure between the depressed and elevated regions was noticed for the PS/PB system, and this was attributed to the edge or shadow effect. The edge effect could be prominent in the phase image if there is a large height difference between the elevated and depressed region. For the 70:30 blend, all the domains are bright and protruding, whereas for the 50:50 and 20:80 blends all the domains are dark and depressed. This observation suggests that the topographic image contrast of the domain is not consistent for different sample compositions. Therefore, the identification of protruded and depressed regions in Figures 1, 2, and 3 as being PS or PEA was not possible from these topographic images.

Another common approach for identifying the composition of the domain and matrix in a phase-segregated system is based simply on changing the sample composition and comparing the areas occupied by the domain and matrix regions.<sup>27,39,35</sup> Using a similar procedure, computer image analysis of 70:30 and 20:80 concentrations was performed to measure the area fraction of the domain regions for each of the blend samples. For these measurements, three  $10 \times 10 \mu\text{m}$  images of each film were analyzed. For the 70:30 blend, the area

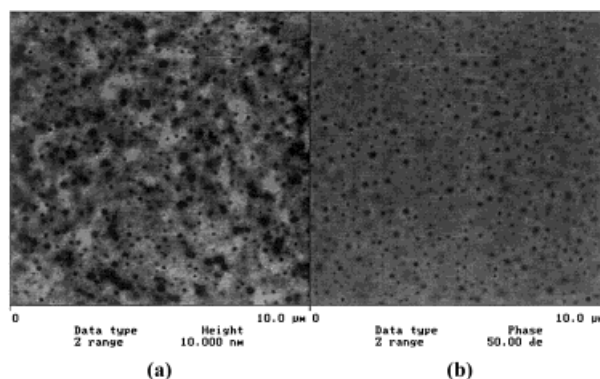


**Figure 3.** Tapping-mode AFM height image (left) and phase image (right) for the 20:80 PEA/PS blend after 24 h of ambient conditioning ( $r_{sp} = 0.7$ ). Contrast variations are 10 nm from white to black for the height image and  $50^\circ$  from white to black for the phase image.

occupied by the bright domains was approximately  $24 \pm 3\%$  of the scan area, whereas that for the 20:80 blend was approximately  $19 \pm 7\%$  of the scan area. Although only a few small areas of each sample were analyzed, the area occupied by domains did not increase proportionately with an increasing PS content but slightly decreased. As the PS content in the blend is increased, phase inversion might occur such that PEA forms domains in the PS matrix. A similar observation has been made in another macromolecular system.<sup>36</sup> From these results, a positive identification of the bright or dark regions in the phase image as PS or PEA regions in the blend based on composition variation was not possible.

A third method for identifying different regions in a heterogeneous system is based on the use of force curve measurements. A force curve is a plot of the deflection of the free end of the AFM probe as a function of  $z$ -piezo motion as the probe approaches, contacts, and withdraws from the sample surface. The force curve can be used to provide information on the local elastic properties. Numerous studies have shown the usefulness of the force curve in distinguishing hard and soft regions in multiphase polymer systems.<sup>21,23,26,27,39</sup> In the present study, force curve measurements were made on the phase-separated regions to identify the domains as PS-rich or PEA-rich regions. We expected the force curve for the PEA region to have a larger hysteresis and deeper trough after unloading compared with that of the PS material because the  $T_g$  values of PEA are much lower than that of PS. Such a behavior would be characteristic of compliant materials and is caused by greater tip penetration, which creates more local inelastic deformation of the sample and higher adhesion forces as a result of the increased tip-sample contact area. However, we noticed that force curve measurements on this system were not always reproducible, and the force curves of domain and matrix regions were difficult to distinguish. Perhaps for the phase-separated regions, a thin layer of the PS resided above and/or below the PEA regions and similarly PEA may have resided above and/or below some PS regions. Also, as commented previously, small regions of PEA were observed in the PS domains. The presence of the matrix phase as tiny droplets within the domains during the late stages of phase separation has been previously observed for other blends.<sup>40</sup> In any case, influences of the glassy PS on the response of a rubbery PEA region and of the rubbery PEA on the response of a

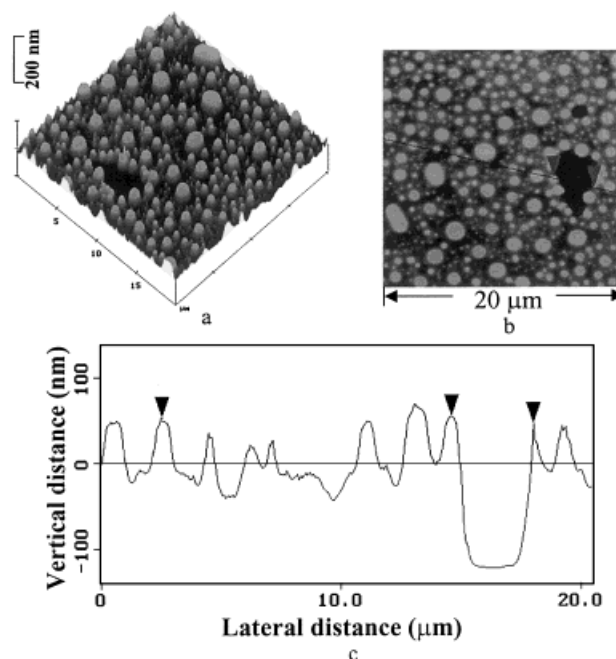


**Figure 4.** (a) A three-dimensional representation of the topography image, (b) tapping-mode height images, and (c) line profile for a 70:30 blend sample after 24 h of ambient conditioning and exposing the film to HCl vapor for 3 h. Contrast variations are 200 nm from white to black for the height images.

glassy PS region might have occurred such that the force curves were not easily distinguishable. Also, the force curves may be influenced by the substrate underneath the thin polymer layer.

#### Chemical Modification of PEA:PS Blend

Because the assignment of the domain and matrix regions of a multiphase system by physical methods is not always possible, a method based on selective chemical modification of one of the components in a two-component system was performed. For example, assignments of the domain and matrix have been made based on exposing diblock and triblock copolymer systems to organic solvents and studying the changes in the image contrast.<sup>37</sup> In our study, an attempt was made to assign the domain and matrix in the blends by exposing the film to an aggressive chemical environment and examining the film by AFM. Figure 4(a) shows a three-dimensional topographic image of the 70:30 PEA/PS film that has been exposed to HCl vapor for 3 h. The thickness of this film was approximately  $150 \pm 20$  nm, as measured by AFM. Changes in the form of pits oc-

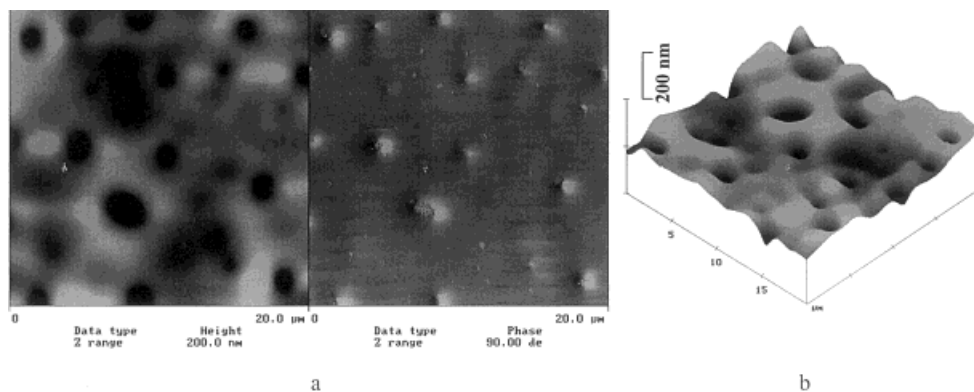


**Figure 5.** (a) Tapping-mode AFM height image (left) and phase image (right) and (b) a three-dimensional of the topography for the PEA film after 24 h of ambient conditioning and exposing the film to HCl vapor for 40 days. Contrast variations are 200 nm from white to black for the height image and  $90^\circ$  from white to black for the phase image.

curred in isolated regions of the matrix, but the overall morphology, size, and shape of the domains were essentially unaltered. The dark regions in the three-dimensional image of Figure 4(a) and the two-dimensional image of Figure 4(b) represent pits that are formed within the heterogeneous structure. A corresponding line profile of the sample is shown in Figure 4(c), which provides the depth and width of the dark region.

To relate the changes resulting from acid exposure in the composition of the PEA/PS blend, PEA and PS cast films were similarly exposed to HCl vapor. The changes observed in the matrix material of the blend were assumed to correspond to changes in either the PEA or PS regions of the film with exposure to HCl vapor. Consequently, any change resulting from hydrolytic degradation should be noticeable in the AFM images of the PEA and PS films.

Although PS is essentially a hydrophobic polymer, it is necessary to determine the susceptibility of PS to acid hydrolysis. To study the susceptibility of the PS film to the same hydrolytic conditions as that for the blend, cast PS film of thickness 200 nm was subject to acid hydrolysis. Little visible change was observed in the topographic image contrast of the PS film after 60 days of exposure: a roughness of  $0.47 \pm 0.04$  nm for the exposed and  $0.45 \pm 0.01$  nm for the unexposed polystyrene film. These results indicate that, under the conditions used in the hydrolysis experiment of the PEA/PS blend, the changes observed in the matrix material were due to the hydrolysis of the PEA regions in the blend and not from the PS domains.

In Figure 5(a), the AFM topographic image (left) and phase image (right) are shown for a  $20 \times 20\text{-}\mu\text{m}$  scan area of a  $110 \pm 10\text{-nm}$  thick PEA cast film that has been exposed to the same acid environment for 40 days. In contrast to the generally smooth surface of the unexposed PEA cast film, the surface of the exposed PEA film shows isolated degradation (dark spots in topographic image). Much of the degradation occurs at certain sites in the form of pits with lateral dimensions from several nanometers to several micrometers, as observed in the three-dimensional topographic image shown in Figure 5(b). The observation of localized degradation at certain areas and not uniformly over the film surface is in good agreement with a recently published chemiluminescence observation that thermooxidation of polypropylene initiates at local active oxidizing centers.<sup>41</sup> Similar observations have been reported for the hydrolysis of a polycarbonate system.<sup>42</sup> The model for this localized hydrolysis is based on the existence of water-sensitive domains that behave differently from the bulk polymer structure.<sup>43</sup> These domains can be polar molecules such as monomers, dimers, or catalysts that did not participate in polymerization. Although the domains are few in an unhydrolyzed polymer, they are believed to represent the initial sites of water sorption, hydrolysis, and degradation. As hydrolysis proceeds, the materials that border the cluster of polar molecules start to degrade through dissolution and/or hydrolysis. The enhanced reactivity of localized domains is consistent with the observations of increases in the

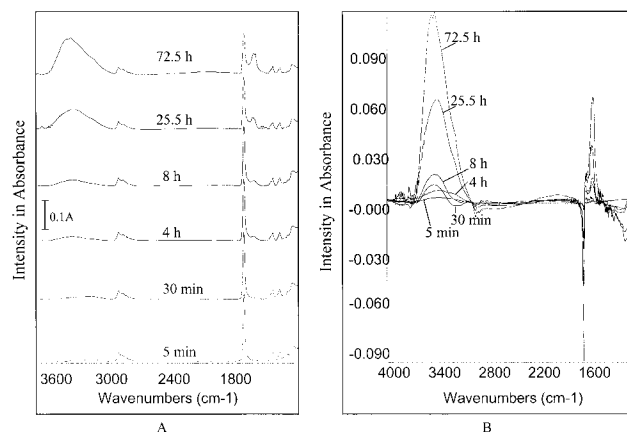


**Figure 6.** (a) Unprocessed and (b) difference FTIR transmission spectra in the 3800–1200-cm<sup>-1</sup> regions showing the effects of exposure of PEA film to HCl vapor.

width and depth of the pits with exposure time and number of isolated pits in the hydrolyzed PEA film.

To verify that the PEA was indeed hydrolyzed during acid exposure, fresh PEA film was subjected to the same acid hydrolysis and temperature conditions (as for the blend), and the composition of the film was studied by FTIR. In Figure 6(a), the FTIR transmission spectra of a spin-coated PEA film on CaF<sub>2</sub> are shown for the region from 3800 to 1200 cm<sup>-1</sup> as a function of exposure time to HCl vapor. A peak attributable to pure PEA is observed at 1732 cm<sup>-1</sup> and is assigned to the ester C=O stretching. The difference spectra [Fig. 6(b)] between the film exposed to different times and the unexposed film were used to measure the ester group consumption and formation of the acid group for the entire 110- ± 10-nm film thickness. Two bands that are attributable to the OH stretching (3400 cm<sup>-1</sup>) and acid C=O stretching (1710 cm<sup>-1</sup>) appear in the difference spectra. This indicates that acid and alcohol were formed on hydrolysis of the PS/PEA film. From the difference spectra, the loss of the ester peak and the growth of acid and alcohol peaks in the PEA/PS film with exposure time can be clearly noticed.

Hydrolysis of PEA is catalyzed by the presence of HCl. Hydrolysis of the polyester (e.g., PEA) film results in the formation of alcohol and carboxylic acid-terminated polymer chains. To study the conversion of ester to acid, the disappearance of the 1732-cm<sup>-1</sup> ester C=O band and the formation of the acid C=O band at 1710 cm<sup>-1</sup> with time

were monitored. Figure 7 depicts a decrease in the intensity of the ester band at 1732 cm<sup>-1</sup> and an increase in the intensity of the acid band at 1710 cm<sup>-1</sup> as a function of exposure time. The released carboxylic acid in the film may enhance the hydrolysis, as reported by several workers.<sup>43</sup> During the initial phase of exposure, a small amount of swelling of the PEA regions in the PEA/PS blend was observed, as evaluated by the change in the topography in the AFM images (data not shown).

Although the timescales of ester conversion, as monitored by FTIR, and that of the morphological alteration of the PEA film as studied by AFM are only qualitatively comparable, all information is consistent with the hydrolysis of PEA in the blend on exposure to HCl vapor and dissolution of the PEA component from the blend leading to the formation of pits. The underlying conclusion from these results is that the changes observed in the PEA film correspond to the changes in the matrix material of the blend when both are exposed to HCl vapor.

With the successful identification of domains and matrix in the chemically heterogeneous polymer blend, the effect of exposure time on the degradation of the 70:30 blend was studied. To quantify the changes in the matrix material with exposure to HCl vapor, the width and diameter of the pit in the 20- × 20-μm image (see Fig. 4) are calculated using AFM analysis software. In Figure 8, the deepening and enlargement progression of the pit are shown as a function of time of

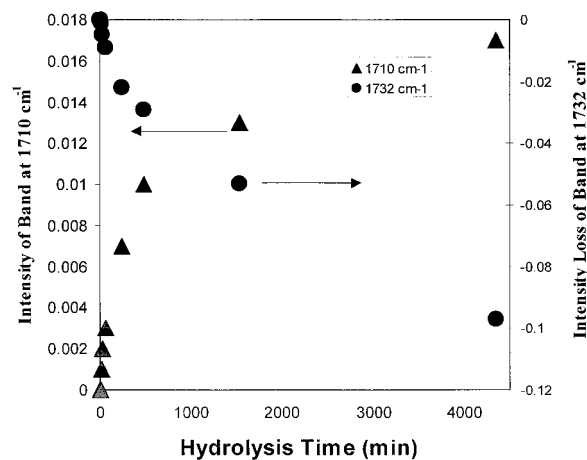


**Figure 7.** The intensity changes of ester carbonyl at 1732 cm<sup>-1</sup> and acid carbonyl at 1710 cm<sup>-1</sup> of a cast PEA film as a function of exposure to HCl vapor at 24 ± 2 °C.

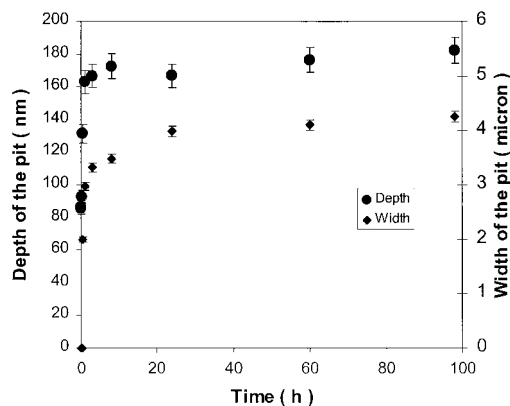


**Figure 8.** Changes in depth and width of a pit in a PEA/PS blend as a function of time exposure to HCl vapor at  $24 \pm 2$  °C.

exposure to HCl vapor. As described previously, the thickness of this film was approximately  $150 \pm 20$  nm. The pit width increased rapidly reaching a value of  $4.2 \mu\text{m}$  within the first 20 h of exposure and then leveled off thereafter. The depth of these pits continued to increase up to 100 nm after 100 h of exposure. These results indicate that the pit not only grew laterally but also through the thickness of the film. In fact, the pit has reached the bare silicon substrate within a very short exposure time, as evidenced in Figure 8(b), in which the entire 150-nm film has been removed.

## DISCUSSION

Evidence from water-contact-angle measurements of the PS ( $\theta = 90^\circ$ ) and PEA/PS blend ( $\theta = 90^\circ$ ) films suggest that the outermost surface of the PEA/PS blend facing the exterior environment is probably rich of the lower surface-energy component (PS). This behavior of the blend is in general agreement with reported findings that the higher surface-energy component is likely to be in contact with the hydrophilic  $\text{SiO}_x$  substrate, whereas the lower surface-energy component is likely to cover the layer of film facing the external environment.<sup>23,35,44</sup> The presence of the thin topmost layer is normally very difficult to detect by AFM alone, unless experimentation is performed at very low tapping-force levels.<sup>35,44</sup> As previously indicated, PEA regions in the blend have degraded under hydrolytic conditions of condensing humidity and HCl vapor. For PEA material in the blend to hydrolyze, HCl and water molecules

must permeate and reach this material in the PEA/PS blend.

Water and HCl can enter the sublayer PEA molecules in the blend either by the breakup of the thin exterior PS layer or by the diffusion through the exterior PS thin layer. For thin films that are few nanometers thick, a dewetting process can occur far below the  $T_g$  of bulk PS, that is, in a room-temperature environment. Numerous studies have reported such dewetting of the thin layer in a polymer blend when the exposure environment is changed from air to water.<sup>38,45–48</sup> Similarly, in the present investigation, such dewetting of the thin PS film outer layer would leave the base layer polymer (PEA) exposed to the external environment for possible hydrolysis or dissolution to occur.<sup>35,44</sup> Another possibility is the transport of water and HCl vapor through defects in the topmost PS layer to the underlying PEA region. Flaws and defects have been reported in thin films of PS specimens.<sup>49,50</sup> The exposure of the underlying PEA region to HCl vapor and condensing humidity is the first step leading to the pit/pathway formation in thin film of PEA/PS blends.

The results of Figure 8(b) suggest that the depth of the pits formed in the blend has reached the film-substrate interface. If the hydrolyzable regions are continuous through the film thickness, simple or autocatalytic hydrolysis of the hydrolyzable PEA is adequate to explain the results observed in Figure 8(b). On the other hand, if the PEA regions are noncontinuous in the PEA/PS blend, hydrolysis of underlying PEA may be hindered by the PS region that is present between the hydrolyzed PEA region and underlying unhydrolyzed PEA regions. However, long-range attractive forces operating between the hydrolyzed PEA region and underlying PEA regions could cause the structural rearrangement of the PS region so as to expose the underlying PEA regions to HCl vapor and condensing humidity for hydrolysis. Such a structural rearrangement as a result of long-range forces has been postulated in several polar/nonpolar systems.<sup>26,35,44</sup> In this scenario, the pathways are formed through a combination of structural rearrangement and hydrolysis. In either case, this mechanism of pit formation in model-coating compounds would result in the formation of pathways through the coatings to the underlying substrate.

Although pit formation was observed in model-coating compounds, the nature of the degradable regions has not been positively identified. Work is

underway to characterize these regions using AFM and chemically modified tips to provide chemical information with nanometer lateral resolution. The direct chemical observation of pathway formation in coatings will help in the design of more durable coatings, which leads to an increase in the service life of polymer-coated structures, such as buildings, bridges, aircrafts, and automobiles.

## CONCLUSIONS

The following conclusions were drawn from the current work:

1. The mapping of chemically heterogeneous regions in model blend films was achieved by chemically modifying one component of the blend followed by AFM imaging.
2. AFM imaging is a valuable tool for quantitative study of pit formation and pit growth in model-coating compounds.
3. During the course of hydrolysis, pits were observed to form locally at the PEA regions of the blend. FTIR evidence suggests that this pit formation corresponds to the hydrolysis of PEA in the blend.
4. Pits were observed to reach the film/substrate interface, creating pathways that could lead to corrosion of the substrate. These pathways could have occurred either by hydrolysis of the continuous PEA regions or by a combination of the hydrolysis of noncontinuous PEA regions and structural rearrangement of PS regions.

This work was supported by the Air Force Office for Scientific Research under Grant No. F49620-98-1-0252.

## REFERENCES AND NOTES

1. Funke, W.; Leidheiser, H.; Dickie, R. A.; Dinger, H.; Fisher, W.; Haagen, H.; Mosle, H. G.; Oechsner, W. P.; Ruf, J.; Scantlebury, J. S.; Svoboda, M.; Sykes, J. M. *J Coat Technol* 1986, 58(741), 79.
2. Mills, D. J.; Mayne, J. E. O. In *Corrosion Control by Organic Coatings*; Leidheiser, H., Jr., Ed.; National Association of Corrosion Engineers: Houston, TX, 1981; p 12.
3. Prini-Fernandez, R.; Corti, H. *J Coat Technol* 1977, 49(632), 62.
4. Mayne, J. E. O.; Mills, D. J. *J Oil Color Chem Assoc* 1975, 58, 155.
5. Wu, C. L.; Zhou, X. J.; Tan, Y. J. *Progr Org Coat* 1995, 25, 379.
6. Miskovic-Stankovic, V. B.; Drazic, D. M.; Teodorovic, M. J. *Corros Sci* 1995, 37, 241.
7. Nguyen, T.; Hubbard, J. B.; Pommersheim, J. M. *J Coat Technol* 1996, 68(855), 45.
8. Corti, H.; Fernandez-Prini, R. *Progr Org Coat* 1982, 10, 5.
9. Kerie, T.; Klein, J.; Binder, K. *Phys Rev Lett* 1996, 77, 1318.
10. Jones, R. A. L.; Norton, L. J.; Kramer, E. J.; Bates, F. S.; Wiltzius, P. *Phys Rev Lett* 1991, 66, 1326.
11. McEvoy, R.; Krause, S.; Wu, P. *Polymer* 1998, 39, 5223.
12. Hasegawa, H.; Hashimoto, T. *Polymer* 1992, 33, 475.
13. Schonherr, H.; Hruska, Z.; Vancso, G. J. *Macromolecules* 1998, 31, 3679.
14. Sauer, B. B.; McLean, R. S.; Thomas, R. R. *Langmuir* 1998, 14, 3045.
15. Magonov, S. N.; Ellings, V.; Whangbo, M. H. *Surf Sci* 1997, 375, L385.
16. Bierwagen, G. P.; Twite, R.; Chen, G.; Tallman, D. E. *Progr Org Coat* 1997, 32, 25.
17. Raghavan, D.; Egwim, K. *J Appl Polym Sci* 2000, 78, 2000.
18. Lieber, C.; Liu, J.; Sheehan, P. *Angew Chem Int Ed Engl* 1996, 35, 687.
19. Rabke, C. E. *Adv Mater Process* 1999, 156(5), 32.
20. Akhremichev, B. B.; Mohny, B. K.; Marra, K. C.; Chapman, T. M.; Walker, G. C. *Langmuir* 1998, 14, 3976.
21. McLean, R. S.; Sauer, B. B. *Macromolecules* 1997, 30, 8314.
22. VanLandingham, M. R.; McKnight, S. H.; Palmese, G. R.; Ellings, V. B.; Huang, X.; Bogetti, T. A.; Eduljee, R. F.; Gillespie, J. W. *J Adhes* 1997, 64, 31.
23. Bar, G.; Thomann, Y.; Whangbo, M.-H. *Langmuir* 1998, 14, 1219.
24. Schmitz, I.; Schreiner, M.; Friedbacher, G.; Grasserbauer, M. *Appl Surf Sci* 1997, 115, 190.
25. Raiteri, R.; Butt, H.-J.; Beyer, D.; Jonas, S. *J Chem Phys* 1, 1999.
26. Raghavan, D.; Gu, X.; Nguyen, T.; VanLandingham, M.; Karim, A. *Macromolecules* 2000, 33(7), 2573.
27. Raghavan, D.; VanLandingham, M.; Gu, X.; Nguyen, T. *Langmuir*, 2000, 16, 2454.
28. Frisbie, C. D.; Rozsnyai, L. F.; Noy, A.; Wrighton, M. S.; Lieber, C. M. *Science* 1994, 265, 2071.
29. Noy, A.; Vezenov, D. V.; Lieber, C. M. *Annu Rev Mater Sci* 1997, 27, 381.
30. Green, J. B. D.; McDermott, M. T.; Porter, M. D.; Siperko, L. M. *J Phys Chem* 1995, 99, 10960.
31. Sinniah, S. K.; Steel, A. B.; Miller, C. J.; Reutt-Robey, J. E. *J Am Chem Soc* 1996, 118, 8925.
32. Wong, S. S.; Woolley, A. T.; Joselevich, E.; Cheung,

- C. L.; Lieber, C. M. *J Am Chem Soc* 1998, 120, 8557.
33. Wong, S. S.; Joselevich, E.; Woolley, A. T.; Cheung, C. L.; Lieber, C. M. *Nature* 1998, 394, 52.
34. Baines, C. D.; Whitesides, G. M. *Angew Chem Int Ed Engl* 1989, 28, 506.
35. Tezuka, Y.; Araki, A. *Langmuir* 1994, 10, 1865.
36. Finot, M. O.; McDermott, M. T. *J Am Chem Soc* 1997, 119, 8564.
37. Elbs, H.; Fukunaga, K.; Stadler, R.; Sauer, G.; Magerie, R.; Krausch, G. *Macromolecules* 1999, 32, 1204.
38. Walheim, S.; Boltau, M.; Mlynek, J.; Krausch, G.; Steiner, U. *Macromolecules* 1997, 30, 4995.
39. Bar, G.; Thomann, Y.; Brandsch, R.; Cantow, H. J.; Whangbo, M. H. *Langmuir* 1997, 13, 3807.
40. Siggin, E. D. *Phys Rev A: At Mol Opt Phys* 1979, 20, 595.
41. Celina, M.; George, G. A.; Billingham, N. C. In *Polymer Durability, Degradation, Stabilization and Lifetime Prediction*; Clough, R. L.; Billingham, N. C.; Gillen, K. T., Eds.; American Chemical Society: Washington, DC, 1996; Vol. 249, p 159.
42. Pryde, C. A.; Hellman, M. Y. *J Appl Polym Sci* 1980, 25, 2573.
43. Rosen, B. *J Polym Sci* 1960, 47, 19.
44. Pientka, Z.; Oike, H.; Tezuka, Y. *Langmuir* 1999, 15, 3197.
45. Reiter, G. *Macromolecules* 1994, 27, 3046.
46. Brochard-Wyart, F.; Debregeas, G.; Fondecave, R.; Martin, P. *Macromolecules* 1997, 30, 1211.
47. Qu, S.; Clarke, C.; Liu, Y.; Rafailovich, M. H.; Sokolov, J.; Phelan, K. C.; Krausch, G. *Macromolecules* 1997, 30, 3640.
48. Suzuki, S.; Green, P. G.; Bumgarner, R. E.; Dasgupta, S.; Goddard, W. A. III; Blake, G. A. *Science* 1992, 257, 942.
49. Linossier, I.; Gaillard, F.; Romand, M.; Feller, J. F. *J Appl Polym Sci* 1997, 66, 2464.
50. Linossier, I.; Gaillard, F.; Romand, M.; Nguyen, T. *J Adhes* 1999, 70, 221.